

Labeling Cells with Silver/Dendrimer Nanocomposites

Wojciech Lesniak¹, Xiangyang Shi¹, Anna Bielinska¹, Katarzyna Janczak¹, Kai Sun² James R. Baker Jr.¹, and Lajos P. Balogh^{1,3,4}

¹Center for Biologic Nanotechnology, ²Electron Microbeam Analysis Laboratory ³Department of Biomedical Engineering, ⁴Macromolecular Science and Engineering, University of Michigan, Ann Arbor, MI 48109

Abstract

We have developed water-soluble, biocompatible, fluorescent, and photostable silver/dendrimer nanocomposites that have a potential to be used for *in vitro* cell labeling. A PAMAM_E5.NH₂ dendrimer was used as a template to prepare first a silver-dendrimer complex in an aqueous solution at biologic pH=7.4. Conversion into nanocomposite was achieved by irradiating the solution of the [(Ag⁺)₂₅-PAMAM_E5.NH₂] complex by UV light to reduce the bound Ag⁺ to zero-valent Ag⁰ atoms, which were simultaneously trapped in the dendrimer network. Results indicate that the {(Ag⁰)₂₅-PAMAM_E5.NH₂} silver/dendrimer nanocomposite forms positively charged single particles of 4-5 nm under the experimental conditions used. The dendrimer nanocomposite proved to be fluorescent. Toxicity testing of {(Ag⁰)₂₅-PAMAM_E5.NH₂} nanocomposite revealed a behavior similar to the template dendrimer. Intracellular internalization of the silver nanocomposite and cell labeling capabilities was confirmed by confocal microscopy.

Introduction

Nanostructured materials have gained increasing attention in the past decades due to their unique properties that provide outstanding opportunities for application in photonics, biology, and medicine. Dendrimer nanocomposites (DNC) [1-3] are nanosized inorganic/organic hybrid composite particles containing topologically trapped guest atoms/molecules/nanocrystals immobilized by dendritic polymer hosts of well-defined size, charge, and terminal functionality. Our goal here is to describe the synthesis, characterization and use of a particular class of silver nanocomposites that can be used as cell labels in *in vitro* experiments. Noble metal nanoparticles have been shown to demonstrate a strong, discrete emission quantum yield that is comparable to bright organic fluorophores, as they exhibit features useful in the biological imaging [4-5]. The properties of metal nanocomposites strongly depend on their size and shape [6-8]. Thus, control of nanoparticle morphology plays an essential role in their future applications. Nanocomposites that can be used in biological systems are required to be water soluble, biocompatible, and photostable. It is well documented that poly(amidoamine) (PAMAM) dendrimers hold great promise in this regard due to their highly regular, symmetrically branched structure with variable surface functionalities, which permits optimization for toxicity. PAMAMs can host inorganic ions or atoms/molecules by forming dendrimer complexes and nanocomposites [9]. Fabrication of metal/dendrimer nanocomposites requires two steps: (1) binding of metal ions to form complexes that act as precursors for consequent nanoclusters formation, and (2) transformation of resulting species to immobilize the preorganized metal ions within dendrimers, as depicted in scheme 1. Using the above principles, we have developed a novel approach for the fabrication of silver/dendrimer nanocomposites that allows to monitor of the chelation of Ag⁺ in dendrimers, estimate their binding capacity and reduce metal ions at a desired pH.

contrary, in the $\text{Ag}^+:\text{PAMAM_E5.NH}_2 = 45:1$ system, the precipitation of unbound Ag^+ ions in the form of silver hydroxide was observed. The hydrolysis of unbound Ag^+ starts at around $\text{pH} = 7.5$, which is evidently visible from the titration curve associated with this sample (triangles). Based on potentiometric data the synthesis of $\{(\text{Ag}^0)_{25}\text{-PAMAM_E5.NH}_2\}$ nanoparticles was designed. Briefly, the $[(\text{Ag}^+)_{25}\text{-PAMAM_E5.NH}_2]$ precursor complex was obtained by mixing aqueous solutions of Ag^+ ions and dendrimer template at 25:1 molar ratio and $\text{pH} 2.5$, which was subsequently increased to $\text{pH} 7.4$ by titrating the system with NaOH solution to get the final dendrimer concentration equal to 1mg/mL . To avoid additional chemical contamination, the dendrimer complex were reduced by UV irradiation. After irradiation, the originally colorless aqueous solution of $[(\text{Ag}^+)_{25}\text{-PAMAM_E5.NH}_2]$ species, became transparent yellow-brown, which confirmed the reduction of Ag^+ to Ag^0 and the formation of $\{(\text{Ag}^0)_{25}\text{-PAMAM_E5.NH}_2\}$ nanocomposite. The UV-Vis spectra of the UV light exposed PAMAM_E5.NH₂, dendrimer template and corresponding silver DNC are presented in figure 1B.

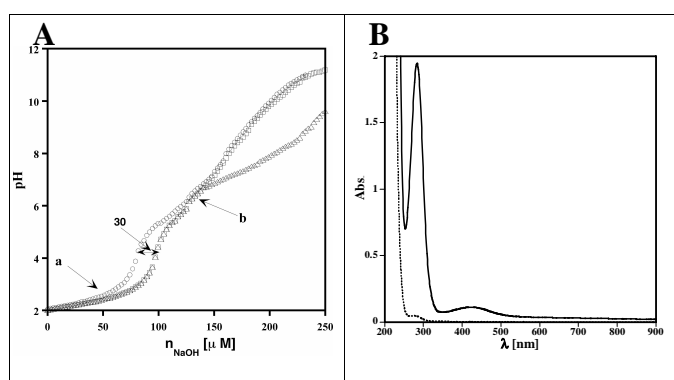


Figure 1. A - Potentiometric titration curves of PAMAM_E5.NH₂ (circles) Ag^+ -PAMAM_E5.NH₂ 30:1 (squares) and Ag^+ -PAMAM_E5.NH₂ 45:1 systems (triangles). B - UV-vis spectra of UV light exposed PAMAM_E5.NH₂ dendrimer (dotted line) and $\{(\text{Ag}^0)_{25}\text{-PAMAM_E5.NH}_2\}$ nanoparticles (solid line), recorded for aqueous samples at $\text{pH} 7.4$.

Solutions of $\{(\text{Ag}^0)_{25}\text{-PAMAM_E5.NH}_2\}$ nanocomposite exhibits two absorbance peaks at 285 and 416 nm. The signal at 416 nm can be assigned as a plasmon peak that results from dipole resonances of aggregated silver nanoparticles. However, absorbance peaks at 285 nm may be related either to single particles or to partially oxidized dendrimer molecules that can form during photolytic reduction of Ag^+ cations [11]. Silver complexes are known to be efficient oxygen transfer catalysts, which is in agreement with a recent report showing increase of this band upon oxidation of PAMAM dendrimers [11]. $\{(\text{Ag}^0)_{25}\text{-PAMAM_E5.NH}_2\}$ nanoparticles were further analyzed by means of dynamic light scattering and zeta potential measurements.

Table 1 Summary of dynamic light scattering and average zeta potential data on $\{(\text{Ag}^0)_{25}\text{-PAMAM_E5.NH}_2\}$ nanocomposite, obtained for a 1 mg/mL aqueous sample at $\text{pH}=7.4$.

Number Weighting Mean Diam [nm]	Volume Weighting Mean Diam [nm]	Intensity Weighting Mean Diam [nm]	Zeta Potential
10.8 (99.6%) ± 0.8	11.1 (83.7 %) ± 1	11.3 (4%) ± 1	+19.45
37.8 (0.4%) ± 2.3	38.7 (15.5%) ± 3.3	40.5 (29.9%) ± 3.8	
	149 (0.8%) ± 18.6	154.6 (66.1%) ± 17.5	

The $\{(\text{Ag}^0)_{25}\text{-PAMAM_E5.NH}_2\}$ nanocomposite particles display relatively narrow size distribution with nanoparticles of hydrodynamic radius, for the most part, small particles and small fraction of higher order of aggregates that exhibit strong light scattering intensity. The particles are positively charged due to the fact that the terminal amino groups of the dendrimer

are still partially protonated at pH 7.4, which also indicates that terminal template functionality determines average charge of nanocomposite. Figure 3 shows a TEM image and related size distribution histograms obtained for the $\{(Ag^0)_{25}\text{-PAMAM_E5.NH}_2\}$ nanoparticles based on evaluation of the images.

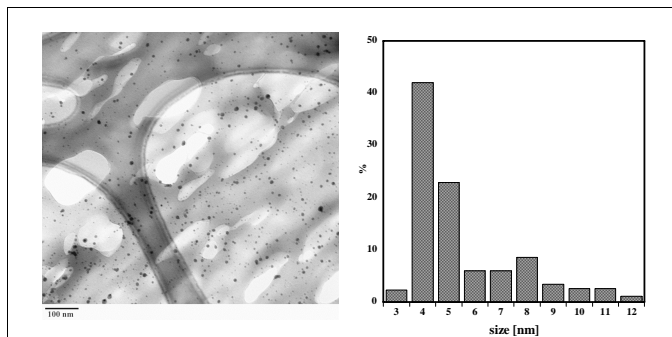


Figure 3. TEM image and related size distribution profiles of $\{(Ag^0)_{25}\text{-PAMAM_E5.NH}_2\}$ nanoparticles was recorded at 92000x magnification. Size distribution histogram was obtained manually using the J-Image computer software.

The histogram indicates that the $\{(Ag^0)_{25}\text{-PAMAM_E5.NH}_2\}$ nanocomposite is predominantly composed of single particles of diameter 4-5 nm. There is a difference between size distribution obtained from DLS and TEM imaging that results from the different underlying principles of the applied methods. First of all, preparation of the samples for TEM required dilution of the solution of $\{(Ag^0)_{25}\text{-PAMAM_E5.NH}_2\}$ by a factor of 2, which may influence the aggregation degree in the system. DLS measurements are collected in solution, whereas for TEM, dry samples are used that may not reflect the exact particle distribution present in solution. Diameters measured from TEM images are only related to the location of the metallic domains in the nanocomposites without observing the organic host of the metal domains, while DLS measurements take into account the whole composite nanoparticle. Finally, due to the resolution threshold of the used particle-sizer (>5 nm), particles with hydrodynamic radius of 11 nm and smaller could be considered as the same fraction close to the lower limit. Figure 4A presents an HRTEM image taken from an arbitrarily selected $\{(Ag^0)_{25}\text{-PAMAM_E5.NH}_2\}_n$ aggregate particle suggesting that in this case a crystalline domain is formed. EDS spectroscopy confirmed that this is Ag domain. The lattice images obtained for the large $\{(Ag^0)_{25}\text{-PAMAM_E5.NH}_2\}$ nanocomposite aggregates indicate that these particles contain either single crystalline or polycrystalline Ag^0 . Figure 4B represent a typical SAED pattern crystalline of Ag domain collected from a number of particles.

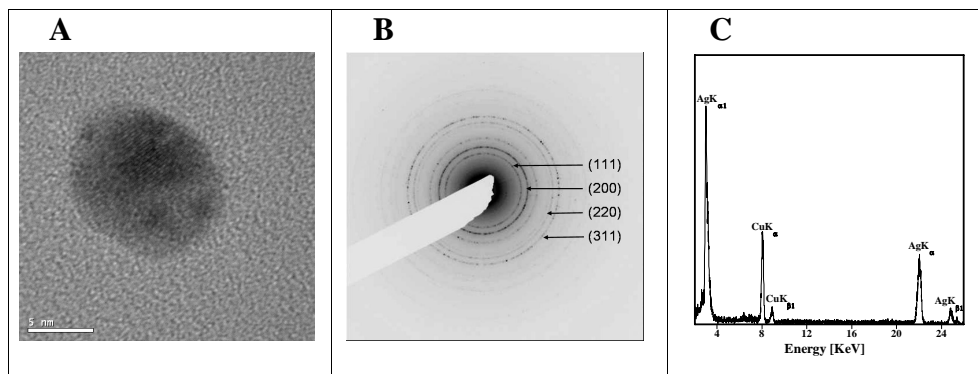


Figure 4. HRTEM image of an aggregate particle; B: selected area electron diffraction (SAED) image, and C: EDS spectrum of the $\{(Ag^0)_{25}\text{PAMAM_E5.NH}_2\}$ nanocomposite.

Silver/dendrimer nanocomposites have been reported to be fluorescent [4-5]. Figure 5 shows the fluorescent spectra of the aqueous solution of $\{(Ag^0)_{25}\text{-PAMAM_E5.NH}_2\}$ that contains fluorescent species that could be excited 340 nm, revealing emissions at 370 and 480 nm. Fluorescence may originate either from the oxidative byproducts, or from the nanosized silver domains (single or aggregated) and may be influenced by the surface aggregation states as well.

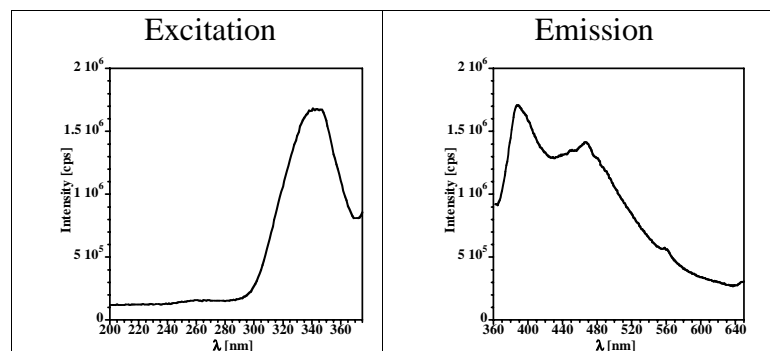


Figure 5. Excitation and emission spectra of the $\{(Ag^0)_{25}\text{-PAMAM_E5.NH}_2\}$ nanocomposite, recorded in aqueous samples at pH =4.

Prompted by the observed fluorescence properties of $\{(Ag^0)_{25}\text{-PAMAM_E5.NH}_2\}$ nanoparticles we further studied this material in terms of its potential application as a biomarker. As the first step, the cytotoxicity of the PAMAM_E5.NH₂ dendrimer template and its related silver DNC was examined in KB cell culture using XTT colorimetric assay of cellular viability (Figure 5A). For PAMAM_E5.NH₂ and $\{(Ag^0)_{25}\text{-PAMAM_E5.NH}_2\}$ similar profiles were obtained, suggesting that dendrimer template determines the toxicity of nanocomposite. Both materials start to exhibit cytotoxicity at concentration around 1000 nM.

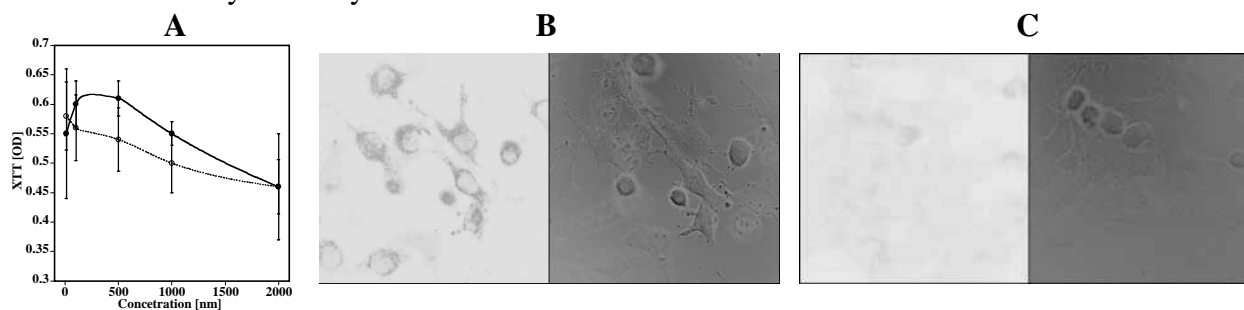


Figure 5. A: Toxicity evaluation of PAMAM-E5-NH₂ dendrimer and (dotted line) $\{(Ag^0)_{25}\text{-PAMAM_E5.NH}_2\}$ (solid line) nanocomposite. KB cells were incubated with nanocomposites at concentration range of 1 and 2000 nM for 2h at 37 °C in PBS buffer (pH 7.4). B: Inverted confocal images of Rat2 cells incubated with $\{(Ag^0)_{25}\text{-PAMAM_E5.NH}_2\}$ nanocomposite at concentration of 500 nM, and C: control cells, recorded in the fluorescence (left panels) and DIC (right panel). Scanning was performed using Zeiss LSM 510 equipped with a UV laser operating at 364 nm and an emission filter that transmits light between 465 and 485 nm.

The cellular uptake and the observability of $\{(Ag^0)_{25}\text{-PAMAM_E5.NH}_2\}$ DNC as a cell label was studied by means of confocal microscopy (Fig. 5 B and C). Both sets of images were collected under the same experimental conditions. Values of PMT and gain power were set to low to decrease the autofluorescence of cells. One can clearly see that cells incubated with $\{(Ag^0)_{25}\text{-PAMAM_E5.NH}_2\}$ nanocomposite exhibit higher intracellular fluorescence, indicating that (a) the nanoparticles are internalized within the cells and are visibly located in the

cytoplasm, and (b) the fluorescence is not quenched. All experiments were reproducible and intracellular enhancement of fluorescence was observed for the cells of each single experiment.

Conclusion

We have demonstrated that potentiometric titration is a right tool to control metal binding by PAMAM dendrimers and to estimate binding capacity of these polymers at given pH values. Irradiation of the aqueous silver ion/dendrimer complex solutions (at pH=7.4) leads to the formation of fluorescent, biocompatible and highly photostable {Ag} dendrimer nanocomposite particles that may be used for cell labeling.

Acknowledgement

This work is financially supported by JTM, Inc.

1. L. Balogh, D.R Swanson., R. Spindler, D.A. Tomalia, Proceedings of ACS PMSE , **77**, 118 (1997)
2. Donald A. Tomalia D.A. and L. Balogh: US Patent No 6,664,315B2, (16 December 16, 2003)
3. Zheng, J.; Dickson, R. M. J. Am. Chem. Soc. 124, 13982 (2004).
4. Peyser, L. A.; Vinson, A. E.; Bartko, A. P.; Dickson, R. M. Science 291, 103 (2001).
5. Mostafa, A.; El-Sayed, M. A. Acc. Chem. Res. 37, 326 (2004)
6. Le Fevre, P.; Magnan, H.; Midoir, A.; Chandesris, D.; Jaffres, H.; Fert, A.; R.; Peyrade, J. P. Surf. Rev. Let. 6, 753 (1999).
7. Peyser, L. A.; Lee, T. H.; Dickson, R. M. J. Phys. Chem. B, 106, 7725 (2002).
8. Balogh, L.; Valluzzi, R.; Hagnauer, G. L.; Laverdure, K. S.; Gido, S. P.; Tomalia, D. A. J. Nanoparticle. Res. 1, 353 (1999).
9. Sun, X.; Dong, S.; Wang, E.; Macromolecules 37, 7105 (2004)
10. Zheng, J.; Stevenson, M. S.; Hikida, R. S.; Van Patten, P. G. J. Phys. Chem. B. 106, 1252 (2002).
11. W. In Lee, Y. Bae, A. J. Bard, J. Am. Chem. Soc. 126, 8358 (2004).